Solution Processable Monosubstituted Hexa-*Peri*-Hexabenzocoronene Self-Assembling Dyes

*Shijie Ren, Chao Yan, Doojin Vak, David J. Jones, Andrew B. Holmes, and Wallace W. H. Wong**

This manuscript is dedicated to the memory of Professor Alan G. MacDiarmid

Molecular organization behavior and visible light absorption ability are important factors for organic materials to be used in efficient bulk heterojunction solar cells applications. In this context, a series of monosubstituted fluorenyl hexa-*peri*-hexabenzocoronene (FHBC) are synthesized with the aim to combine the self-association property of the FHBC unit with broadened light absorption of a small molecule organic dye, bisthienylbenzothiadiazole (TBT). Optical and electrochemical properties of the FHBC compounds vary according to their structures. Introduction of a TBT unit into the FHBC system broadens the absorption. All of the FHBC compounds show strong π–π intermolecular association in solution. X-ray scattering measurements on thermally extruded filaments and thin films showed ordered alignment of these compounds in the solid state. In atomic force microscopy experiments, nanoscale phase separation is observed in thin films of FHBC and fullerene derivative blends. Solar cell devices with these compounds as donors are fabricated. FHBC compounds with the TBT unit show higher short circuit current while the high open circuit voltages are maintained. With C_{60} derivative as acceptor, power conversion efficiency of 1.12% is achieved in the unoptimized solar cell devices under simulated solar irradiation. The efficiency was further improved to 1.64% when C_{70} derivative was used as the acceptor.

1. Introduction

The growing demand for renewable and environmentally friendly energy sources has stimulated scientific research for efficient, low-cost photovoltaic devices. Since the pioneering work of Tang in 1986,[1] intensive interdisciplinary research carried out in the field of organic solar cells (OSC), especially in the last decade, has led to great improvements in terms of the power conversion efficiency (PCE) as well as device stability and durability.[2] So far, bulk heterojunction solar cells (BHJSC), whose active layers are composed of an interpenetrating network of electron donors and acceptors, have played a leading role in realizing higher efficiencies.[3] Recently, some new low bandgap polymers were reported and exhibited PCE in excess of 7% due to strong broadened absorption in the visible to near infrared range and higher charge carrier mobility.[4] It is estimated that the PCE of polymer solar cells can be improved further by implementing new materials and exploring new device architecture.[5]

In recent years, soluble and conjugated small molecule or oligomeric electron donors have emerged as promising alternatives to their polymer counterparts, with some obvious merits such as having a more straightforward synthesis, ease of purification and characterization, less batch-to-batch variation in both structures and properties, and intrinsic monodispersity.[6] Hexa-*peri*-hexabenzocoronene (HBC) is a graphitic aromatic molecule built up from 13 fused six-membered rings. This compound, and functionalized derivatives thereof, can self-assemble into columnar structures giving rise to ordered morphology in the solid state.[7] Efficient charge transport through these materials is a direct result of the ordered nanostructures, making them potentially very useful building blocks for application in organic electronics.[8] Currently, most HBC derivatives rely on alkyl or alkoxy chains at the periphery for solubility, which limits the potential for further functionalization. Moreover, the peripheral long alkyl or alkoxy chains of the HBC derivatives adversely affect charge transport in the bulk material as they can create an insulating domain around the π–π stacked columnar core.[7a,8d,8e] Recently, our group reported the synthesis and optoelectronic properties of a series of highly soluble functional HBC derivatives carrying conjugated substituents.[9] The 9,9-dioctylfluorenyl hexa-*peri*-hexabenzocoronene (FHBC) moiety has emerged as a material with excellent solubility and the potential for further derivatization. Compounds from 2,5- or 2,11-bis-substituted FHBC compounds showed retained self-association properties while compounds from 2,5,8,11,14,17-hexasubstituted FHBC did not.[9b,9c,9e] Interestingly, monosubstituted HBC compounds are rare in the literature due to poor solution processability.[9f] By taking advantage of the 9,9-dialkylfluorene unit, soluble monosubstituted HBC derivatives were synthesized and thoroughly characterized.

Although self-assembly of the FHBC compounds can help to form good morphology and improve the charge mobility of

Dr. S. Ren, Dr. C. Yan, Dr. D. Vak, Dr. D. J. Jones, Prof. A. B. Holmes, Dr. W. W. H. Wong
School of Chemistry
The University of Melbourne
Bio21 Institute, 30 Flemington Road,
Parkville, Victoria 3010, Australia
E-mail: wwhwong@unimelb.edu.au

DOI: 10.1002/adfm.201102141

the materials, absorption edge of these compounds remains less than 500 nm. For efficient BHJSCs application, more intensive and broader absorption of these compounds is necessary. Bisthienylbenzothiadiazole (TBT) based compounds or polymers have emerged as one of the most studied classes of small molecule dye compounds used in BHJSCs due to their broad light absorption and planar structure.[10] In this work, two new FHBC derivatives and three FHBC-TBT hybrids are presented. Apart from synthesis and characterisation of these materials, detailed studies on their photophysical and self-association properties are carried out. Preliminary results on BHJSC devices with these compounds as the electron donor material are also reported.

2. Results and Discussion

2.1. Synthesis and Characterization

Synthesis of monosubstituted FHBC compound **F1**, with two dioctylfluorene solubilizing groups, started from the Sonogashira coupling reaction of phenylacetylene **1** and 1-bromo-4-iodobenzene **2** (**Scheme 1**). Suzuki coupling reaction between acetylene **3** and fluorene boronic ester **4** gave rise to the fluorenyl phenylacetylene **5**, which underwent a Diels–Alder reaction/CO extrusion with cyclopentadienone **6** to give the hexa-arylbenzene derivative **7**. Iodination of **7** afforded the FHBC precursor compound **8**, which was oxidatively cyclized to give the first generation of monosubstituted FHBC compound **9**. Interestingly, there is a significant solubility difference between monosubstituted FHBC **9** and the 2,11-bis(fluorenyl) derivatives reported previously.[9a] One 9,9-dioctylfluorenyl substituent does not provide sufficient solubility to the strongly aggregating HBC core. As a result, FHBC **9** could not be fully characterized and was not examined further in this study.

Starting from compound **8**, a second dioctylfluorene unit was installed to give monosubstituted FHBC compound **12** through a similar sequence of reactions including Suzuki coupling, iodination and oxidative cyclization. Compound **12** was readily soluble in hot solvents such as toluene or chloroform. Borylation of compound **12** gave rise to the boronic ester **13**,

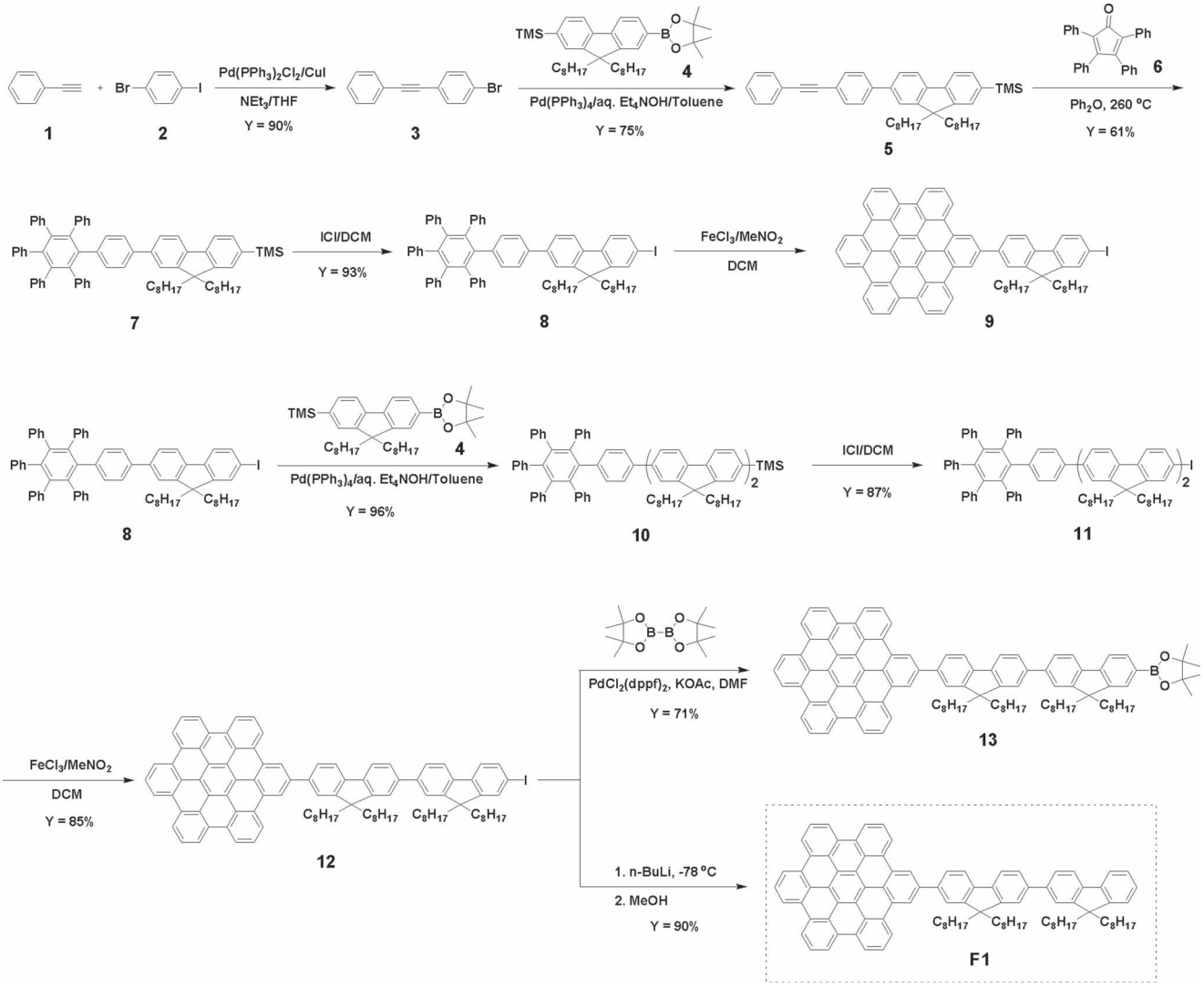

Scheme 1. Synthesis of FHBC compound **F1**.

and the removal of the iodo substituent afforded monosubstituted FHBC **F1**. A similar sequence of reaction were employed for the synthesis of various FHBC compounds bearing oligomeric tris(fluorenyl) substituents **16**, **17** and **F2** (**Scheme 2**). These derivatives showed good solubility in common organic solvents, such as dichloromethane, chloroform and tetrahydrofuran (THF) at room temperature. 2,11-Bis-substituted FHBC compounds **18**,[9a] **19**,[9d] and **20**[9c] were prepared according to previous reports (**Scheme 3**).

Bisthienylbenzothiadiazole (TBT) derivative **21** was obtained by previously reported procedures (Scheme 3).[11] Suzuki coupling reactions between different FHBC boronic esters **13**, **17**, and **19** and the TBT derivative **21** gave rise to the FHBC-TBT compounds **F3**, **F4**, and **F5** (Scheme 3). All of the new compounds synthesized were fully characterized with a range of methods, including as ^{1}H NMR, ^{13}C NMR spectra, mass spectrometry, and elemental analysis, as detailed in the Experimental Section (NMR spectra in Supporting Information Figure S1–8).

Monosubstituted FHBC compounds **F1** and **F2** and the FHBC-TBT materials **F3**, **F4**, and **F5** showed good thermal stability in thermal gravimetric analysis (TGA) experiments (**Table 1**, TGA curves in Supporting Information Figure S9), with 5% weight loss temperatures at 401, 374, 421, 422, and 415 °C respectively. In differential scanning calorimetry (DSC) experiments, glass transitions at round 132 °C were observed for these FHBC compounds (Table 1, DSC curves in Supporting Information Figure S10–14).

2.2. Optical and Electrochemical Properties

Optical properties of the FHBC compounds and their derivatives were measured by UV-vis and photoluminescence (PL) spectroscopy. In chlorobenzene solutions (5×10^{-3} mg mL^{-1}), FHBC derivatives **F1** and **F2** showed maximum absorption at 364 nm and a shoulder peak at about 390 nm, presumably due to the π–π* transition of the fluorene oligomer and the HBC-fluorene extended conjugation respectively (**Figure 1**a). For the FHBC compounds with one TBT unit, **F3** and **F4**, the maximum absorption peak was still at around 364 nm; however, the shoulder peak at 390 nm was enhanced compared with that of **F1** and **F2**. The absorption edge of compounds **F3** and **F4** extended to 515 nm, whereas that of **F1** and **F2** was at about 430 nm. Not surprisingly, **F5** with two TBT units showed broader absorption up to 525 nm, with an additional absorption peak at 422 nm, which can be attributed to the interaction between FHBC and TBT units. In the solid state, the UV-vis absorption of these compounds showed a shift to longer wavelength compared with their corresponding solution absorption spectra (Figure 1b). For example, the absorption onset of **F5** thin film was at 575 nm, a 50 nm red-shifting compared with its absorption onset in chlorobenzene solution. This red-shift in absorption was an indication of aggregation in the solid state. Similar to the absorption in solution, the introduction of TBT units broadened absorption spectra of the FHBC compounds and a new absorption peak appeared for **F5**. It can be seen from these results that the addition of TBT units can broaden the absorption of the FHBC compounds effectively, which should be advantageous for the solar cell application.

In chlorobenzene solutions, when excited at 364 nm, FHBC derivatives **F1** and **F2** showed maximum emission peak at 490 nm (**Figure 2**a). Under the same conditions, the emission peak at 490 nm of compounds **F3** and **F4** decreased significantly and a new emission peak from TBT unit at 600 nm emerged. When two TBT units were added to the FHBC system, compound **F5**

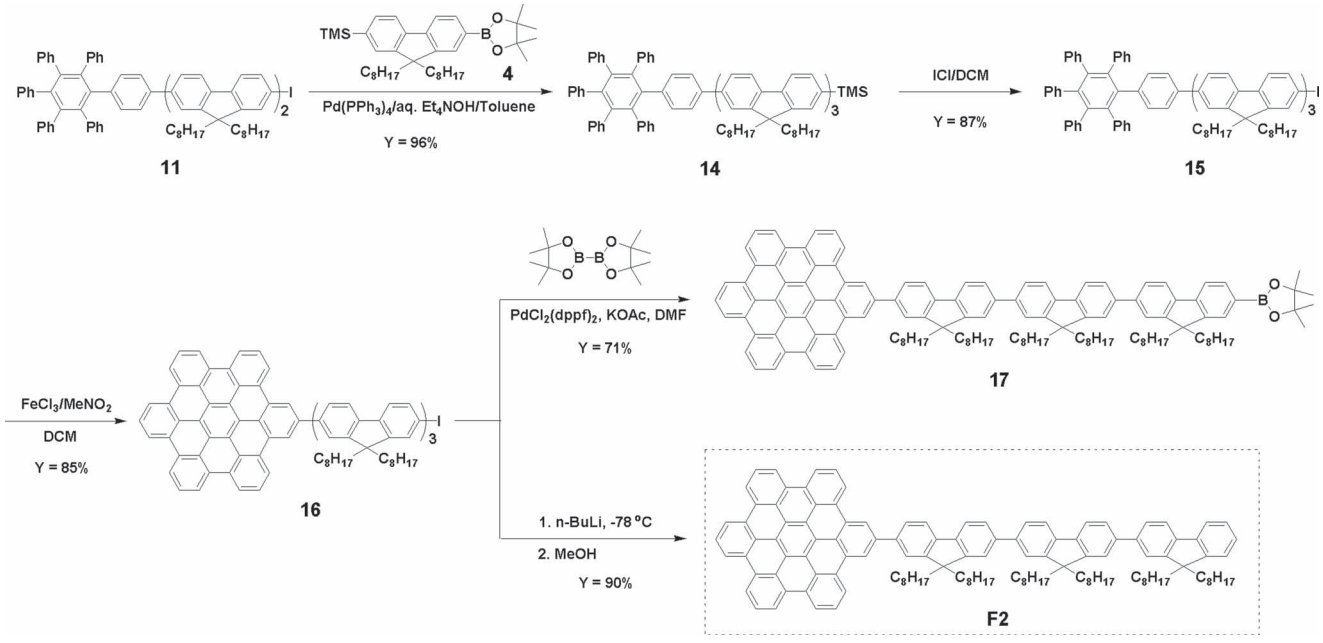

Scheme 2. Synthesis of monosubstituted FHBC compound **F2**.

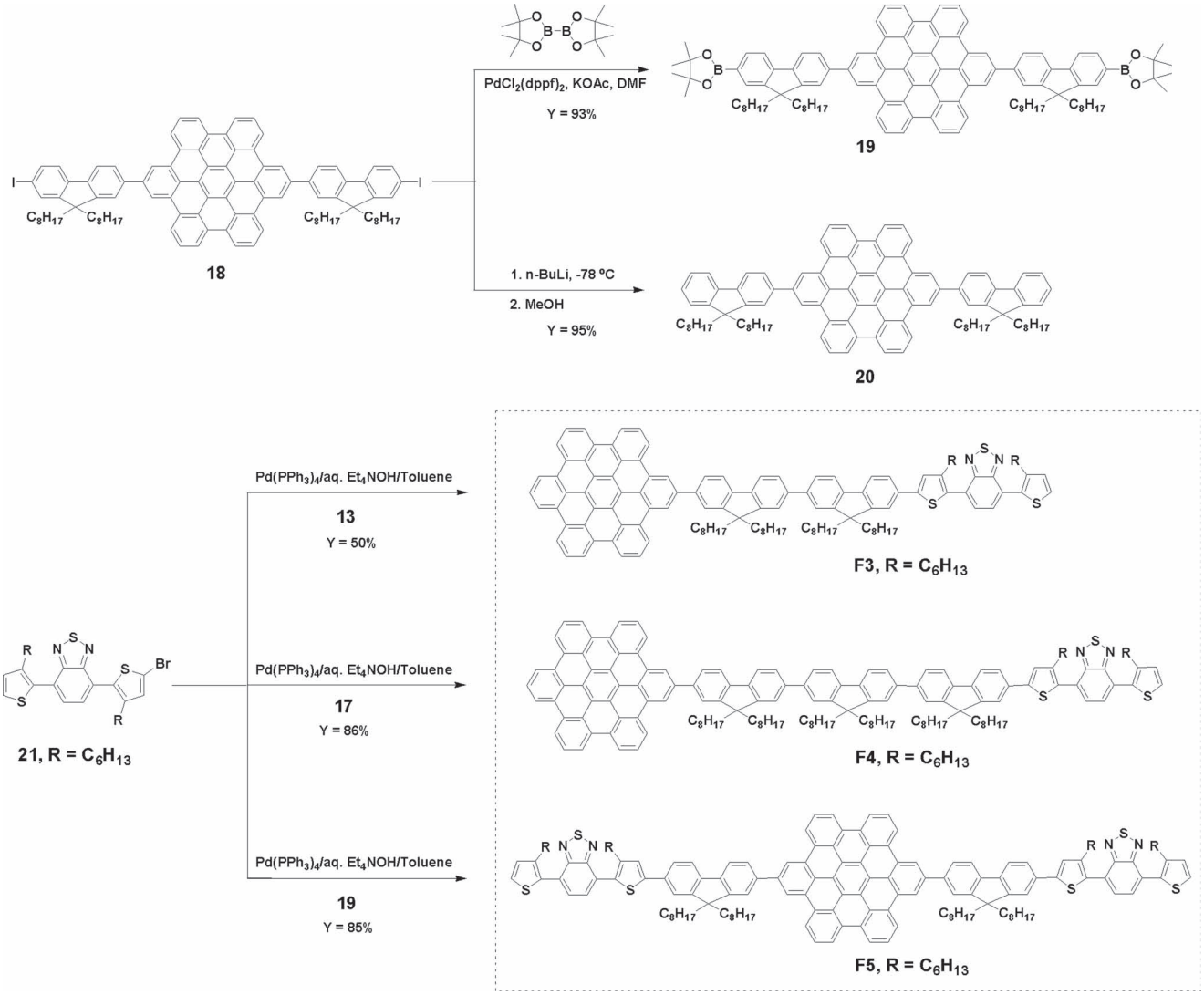

Scheme 3. Synthesis of FHBC compounds **F3**, **F4**, and **F5**. The synthesis of the 2,11-bis-substituted FHBC compounds **19**[9d] and **20**[9c] and the TBT derivative **21**[11] have been reported previously.

showed only one PL emission peak at 601 nm, which indicated that intramolecular energy transfer occurred in the system when excited. In the solid state, all the five compounds showed an emission peak at around 600 nm (Figure 2b). The maximum emission wavelength of compounds **F1** and **F2** shifted significantly to longer wavelength compared with that in solution,

Table 1. Summary of thermal (TGA and DSC), photophysical data (UV-vis and PL) and electrochemical data for FHBC compounds **F1** to **F5**.

Compounds	T_{deg} [°C][a]	T_g [°C][b]	λ_{abs}^{max} [nm]		λ_{em}^{max} [nm]		E_g^{Opt} [eV][e]	E_{ox}^{onset} [V][f]	HOMO [eV][g]	LUMO [eV][h]
			Solution[c]	Film[d]	Solution[c]	Film[d]				
F1	401	132	364 (1.9)	366	489	601	2.88	0.82	–5.62	–2.74
F2	374	133	364 (2.1)	370	488	587	2.88	0.79	–5.59	–2.71
F3	421	132	363 (1.7)	371	488, 601	589	2.43	0.78	–5.58	–3.15
F4	422	132	364 (2.3)	381	488, 601	591	2.43	0.71	–5.51	–3.08
F5	415	135	370 (1.8); 422 (0.8)	381; 448	601	595	2.34	0.70	–5.50	–3.16

[a]Degradation temperature (T_{deg}) observed from TGA corresponding to 5% weight loss at 10 °C min^{-1} under nitrogen flow; [b]Glass transition temperature (T_g) from DSC with heating/cooling rate at 20 °C min^{-1}; [c]Measured in chlorobenzene solution (5×10^{-3} mg mL^{-1}) and extinction coefficient ($\times 10^5$ M^{-1} cm^{-1}) in brackets; [d]Spin-coated from chlorobenzene solutions (25 mg mL^{-1}); [e]Estimated from the UV-vis absorption edge in chlorobenzene solutions; [f]Cyclic voltammograms measured in dichloromethane, 1×10^{-3} M, Bu_4NPF_6 (0.1 M), 295 K, scan rate = 100 mV s^{-1}, Ag/Ag$^+$ reference electrode; [g]Determined from $E_{HOMO} = -(E_{ox}^{onset} + 4.80)$ [eV]; [h]Determined from $E_{LUMO} = E_{HOMO} + E_g^{Opt}$ [eV].

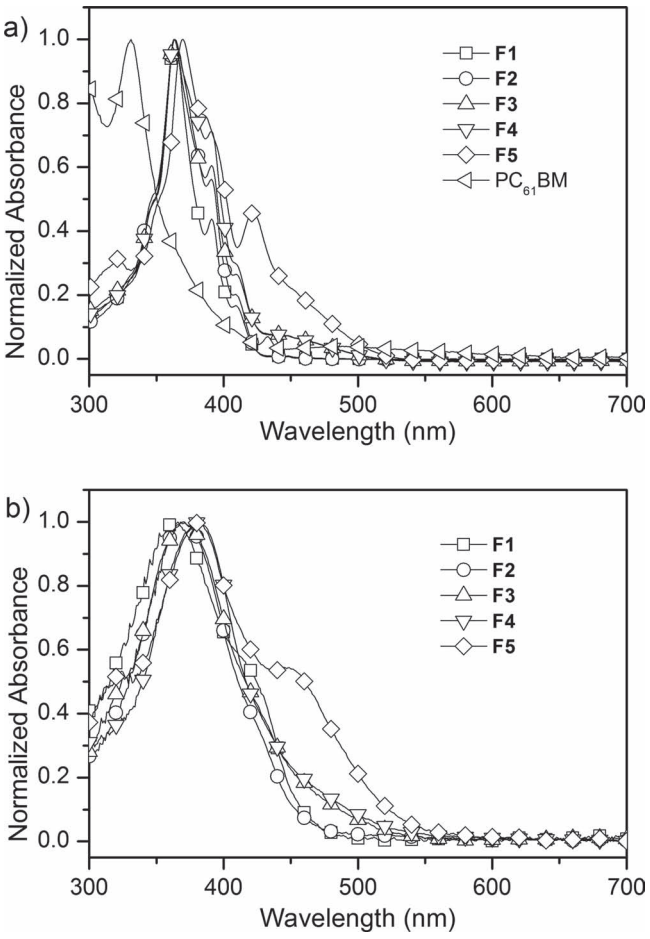

Figure 1. UV-vis spectra of FHBC derivatives **F1** to **F5** a) in chlorobenzene solution (5×10^{-3} mg mL^{-1}) and b) in thin films.

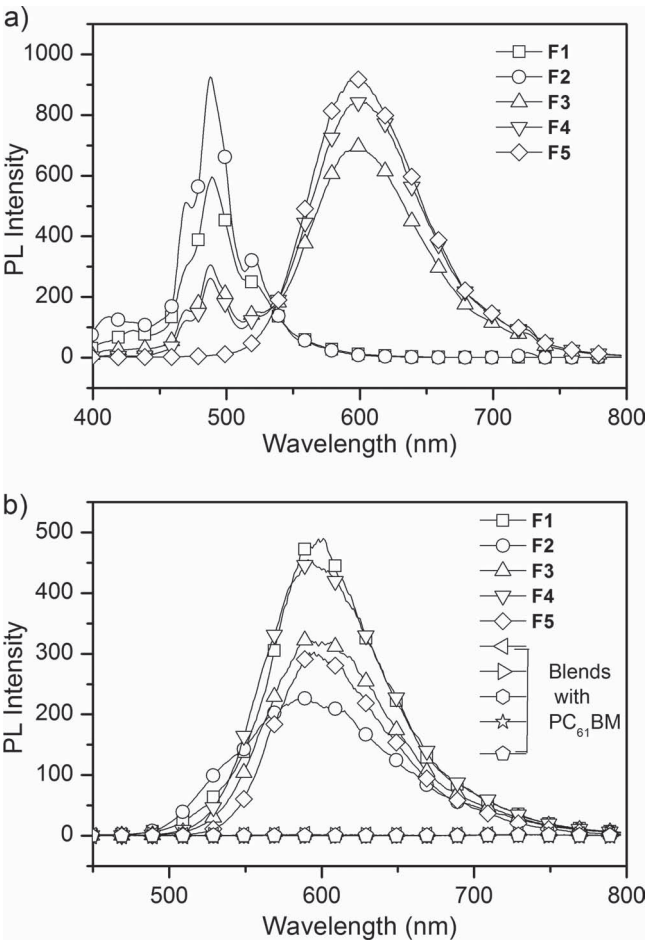

Figure 2. PL spectra of FHBC derivatives **F1** to **F5** a) in chlorobenzene solutions (5×10^{-3} mg mL^{-1}) and b) in the thin films.

probably due to the strong molecular aggregation in the solid state.

Optical bandgaps of the FHBCs were estimated from the onset wavelength of their optical absorption in chlorobenzene solutions, as summarized in Table 1. The energy gap between the highest occupied molecular orbital (HOMO) and the lowest unoccupied molecular orbital (LUMO) of **F1** and **F2** were both around 2.88 eV, while the TBT-containing derivatives **F3** and **F4** had a smaller energy gap of 2.43 eV. Introduction of two TBT units into the FHBC system lowered the HOMO-LUMO gap further to 2.34 eV. Cyclic voltammetry (CV) was used to study the energy levels of the FHBC compounds (CV curves are illustrated in the Supporting Information Figure S15,S16). For solutbility reasons, the measurements were performed in chlorobenzene solutions (10 mM) with tetrabutylammonium hexafluorophosphate as electrolyte (0.1 M). The CVs were recorded with a scan rate of 0.1 V s^{-1} using a glassy carbon working electrode with a platinum counter electrode and a pseudo Ag/Ag$^+$ electrode as referemce. The ferrocene/ferrocenium redox couple was recorded in the same solvent system to serve as an internal standard. All the compounds exhibited electrochemical oxidation behavior with the onset located at 0.70–0.82 eV versus Ag/Ag$^+$. The HOMO and LUMO energy levels of these oligomers were then calculated (Table 1). Energy level diagrams of the FHBC compounds derived from electrochemical and UV-vis absorption data are shown in **Figure 3**. The energy level information suggests all five FHBC derivatives are suitable candidates as electron donor materials in bulk heterojunction solar

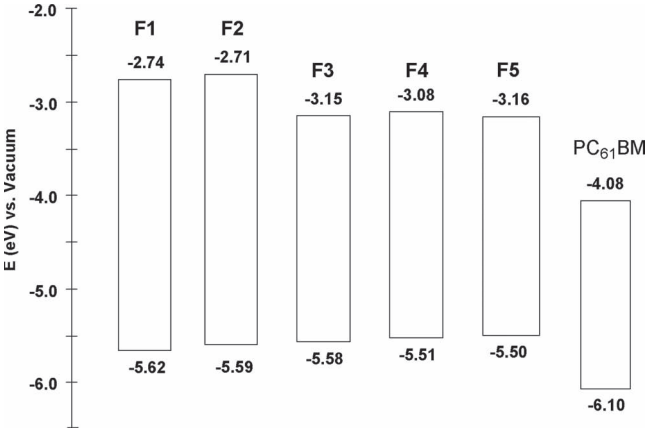

Figure 3. Energy level diagram of FHBC compounds and $PC_{61}BM$.

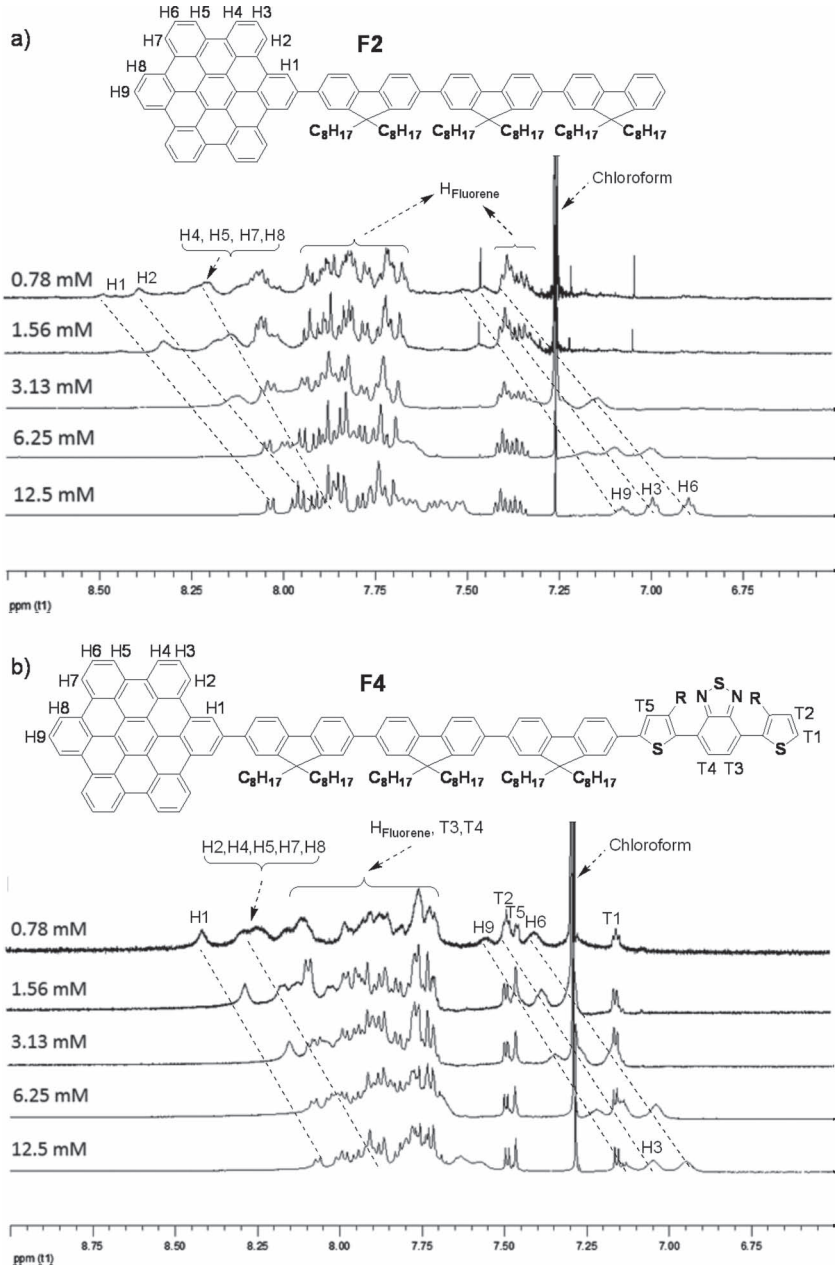

Figure 4. Concentration dependent ^{1}H NMR spectra of FHBC derivatives a) **F2** and b) **F4** ($CDCl_3$ at 20 °C).

cells with [6,6]-phenyl-C_{61}-butyric acid methyl ester ($PC_{61}BM$) as the electron acceptor. The addition of TBT unit to the FHBC system lowered the LUMO energy levels of these compounds effectively, while HOMO levels of the FHBC compounds were not changed significantly. It is known that open-circuit voltage (V_{oc}) of BHJ solar cells is determined by the energy level difference between the LUMO level of acceptor and the HOMO level of the donor.[5a,12] Therefore, the introduction of TBT will not significantly change the V_{oc} while the HOMO-LUMO energy gap of the FHBC compounds is lowered. Energy or charge transfer between the FHBC donor materials and the fullerene acceptor can be observed by fluorescence quenching studies. Fluorescence of the FHBC donor materials were completely quenched when blended with $PC_{61}BM$ (FHBC:$PC_{61}BM$ = 1:2 w/w) in thin films deposited by spin coating (Figure 2b). This was another indication of the compatibility of the donor and acceptor materials for use in solar cell devices.

2.3. Self-Assembling Properties and Solid State Morphology

In previous reports, we found that despite the steric hindrance of the aromatic fluorenyl substituents, a range of FHBC compounds still showed strong self-association of the HBC core in solution and in the solid state.[9] To examine the π–π stacking properties of the FHBC derivatives in this study, NMR spectroscopic studies were performed. ^{1}H NMR spectra of the aromatic region of compounds **F2** and **F4** are shown in **Figure 4**. Peak assignments were made primarily on the basis of the multiplicity of the peaks and by comparison with spectra of known material. It can be seen from Figure 4 that the ^{1}H NMR spectra of both **F2** and **F4** showed concentration dependence. The protons assigned to the HBC core (H1–9) shift significantly up field with increasing concentration due to a shielding effect caused by π–π stacking between FHBC molecules. The protons on the fluorene moiety closest to the HBC core also shift up field with increasing concentration, although not as significantly as the protons on the HBC core. However, there is little change in the resonances associated with the protons of the peripheral fluorene and TBT units in these compounds, indicating the π–π interaction of the FHBC cores with the peripheral units was most likely arranged in a staggered manner,[13] as was observed in previous systems.[9c] Compound **F5** showed similar concentration dependent NMR behavior (Supporting Information Figure S17).

In order to investigate the organization in the solid state, X-ray diffraction (XRD) experiments were performed. Two-dimensional wide-angle X-ray scattering (2D-WAXS) experiments were carried out on thin filaments of compounds at the SAXS/WAXS beamline of the Australian Synchrotron with a wavenumber of 0.62 Å^{-1}. Filaments of 0.7 mm diameter were prepared by thermal extrusion and were mounted vertically towards the 2D detector. A typical well-ordered columnar organization[14] was found for all the compounds. **Figure 5**a shows a 2D diffraction pattern for **F2** (similar diffraction patterns for the other compounds are shown in the Supporting Information Figure S18). The diffractions of those compounds in the meridional direction revealed a π-stacking distance of 0.34 nm for co-facially arranged discs, which is

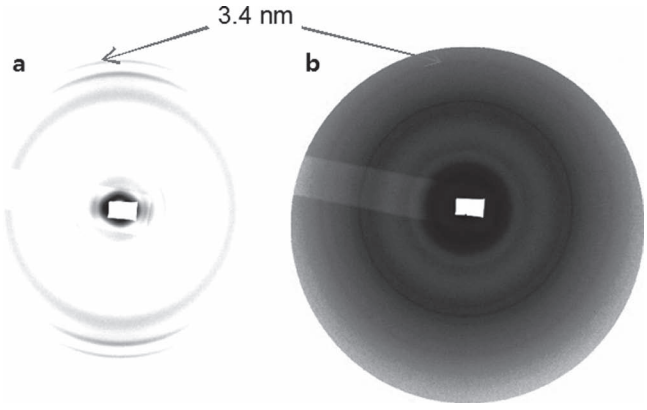

Figure 5. 2D-WAXS patterns of a) fiber diffraction of **F2** and b) diffraction of blend thin film of **F2**/$PC_{61}BM$ (1:2 w/w).

consistent with our previous reports on HBC core materials.[9b,9c] This kind of ordered columnar structure is maintained after the FHBC derivatives were blended with $PC_{61}BM$ (1:2 w/w) in thin films (Figure 5b). The well-ordered structure in the solid state could improve the performance of resultant solar cell devices.

2.4. Bulk Heterojunction Solar Cells

With all the optoelectronic and self-organization studies presented above, the FHBC derivatives appeared to be promising candidates as the electron donor material in bulk heterojunction solar cells. Devices with the structure ITO/PEDOT:PSS/FHBC:fullerene(1:2 w/w)/TiO_x/Al (ITO, indium tin oxide; PEDOT, poly(3,4-ethylenedioxythiophene); PSS, poly(styrenesulfonate)) with the FHBC compounds as electron donors and fullerene derivatives as electron acceptors were fabricated and characterized. The active layer was deposited by spin coating from chlorobenzene solutions and the thickness was typically between 60 and 70 nm. TiO_x layers were introduced as an optical spacer and a hole blocker by following literature procedures.[10e] In general, all devices showed good diode-like behavior in the dark, and appropriate photovoltaic effects under simulated AM 1.5 G illumination. **Table 2** summarizes the

Table 2. Device performance of BHJ solar cells with active layers consisting of 1:2 donor/acceptor blends. Active layer thickness was 60-70 nm. Efficiency values quoted in this table are averages over a number of devices.

Donor	Acceptor	J_{sc} [mA cm^{-2}]	V_{oc} [V]	Fill factor	PCE [%]
F1	$PC_{61}BM$	1.62	0.77	0.42	0.52
F2	$PC_{61}BM$	1.64	0.87	0.59	0.84
F3	$PC_{61}BM$	2.64	0.82	0.49	1.06
F4	$PC_{61}BM$	2.67	0.85	0.49	1.12
F5	$PC_{61}BM$	2.67	0.99	0.34	0.90
F5	$PC_{71}BM$	5.07	0.96	0.34	1.64
20[a)]	$PC_{61}BM$	1.87	0.93	0.45	0.78

[a)]The device performance of compound **20** shown here was obtained from ref. [9c].

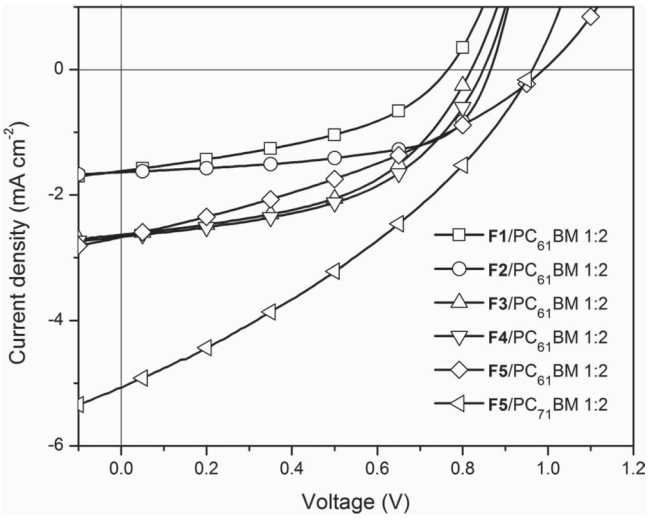

Figure 6. Current density–voltage curves of devices containing FHBC compounds **F1** to **F5**.

device performance of the various solar cells and the following characteristic parameters are given: short-circuit current density (J_{sc}), open-circuit voltage (V_{oc}), fill factor, and power-conversion efficiency (PCE). The device performance of 2,11-bis(fluorenyl) derivative **20** reported previously is also shown in Table 2 for comparison with materials in this study.[9c] The current density to voltage curves of these devices are shown in **Figure 6**.

There is a clear correlation between current density and the spectral absorption of these compounds in the series of devices. The J_{sc} of devices containing FHBC compounds with TBT units **F3**, **F4** and **F5** increased substantially compared to **F1** and **F2** as a result of the broadened light absorption. All devices exhibit a relatively high V_{oc} compared with the conjugated polymer-based solar cell devices, derived from the low-lying HOMO energy levels of these FHBC materials. Meanwhile, V_{oc} of these devices did not change significantly with the introduction of the TBT moieties, as predicted from the energy level measurements.

The addition of TBT units not only broadens the light absorption but also affects the self-organized structure in the blends of FHBC/$PC_{61}BM$, as indicated by atomic force microscopy (AFM) in **Figure 7**. Thin films of FHBC/$PC_{61}BM$ blends, deposited from chlorobenzene solution by spin coating, were probed by tapping mode AFM. Nanoscale phase separation was observed in all those blend thin films. The surface roughness of films containing compounds **F1**, **F2**, and **20** were much higher than that of the films containing compounds **F3**, **F4**, and **F5**. The smaller phase separation for TBT unit contained compounds provided more interface between donor and acceptor, which resulted in more effective charge separation and transport.

The use of [6,6]-phenyl-C_{71}-butyric acid methyl ester ($PC_{71}BM$) instead of $PC_{61}BM$ can normally boost the current generated from solar cell devices as a result of higher absorptivity of $PC_{71}BM$.[15] In this study, replacing $PC_{61}BM$ for $PC_{71}BM$ for the **F5** based device resulted in a nearly doubled J_{sc}, which increased the power conversion efficiency of the device from 0.9% to 1.64%. The spectral response of the devices is shown in **Figure 8**. It is clear from this data that both devices harvest

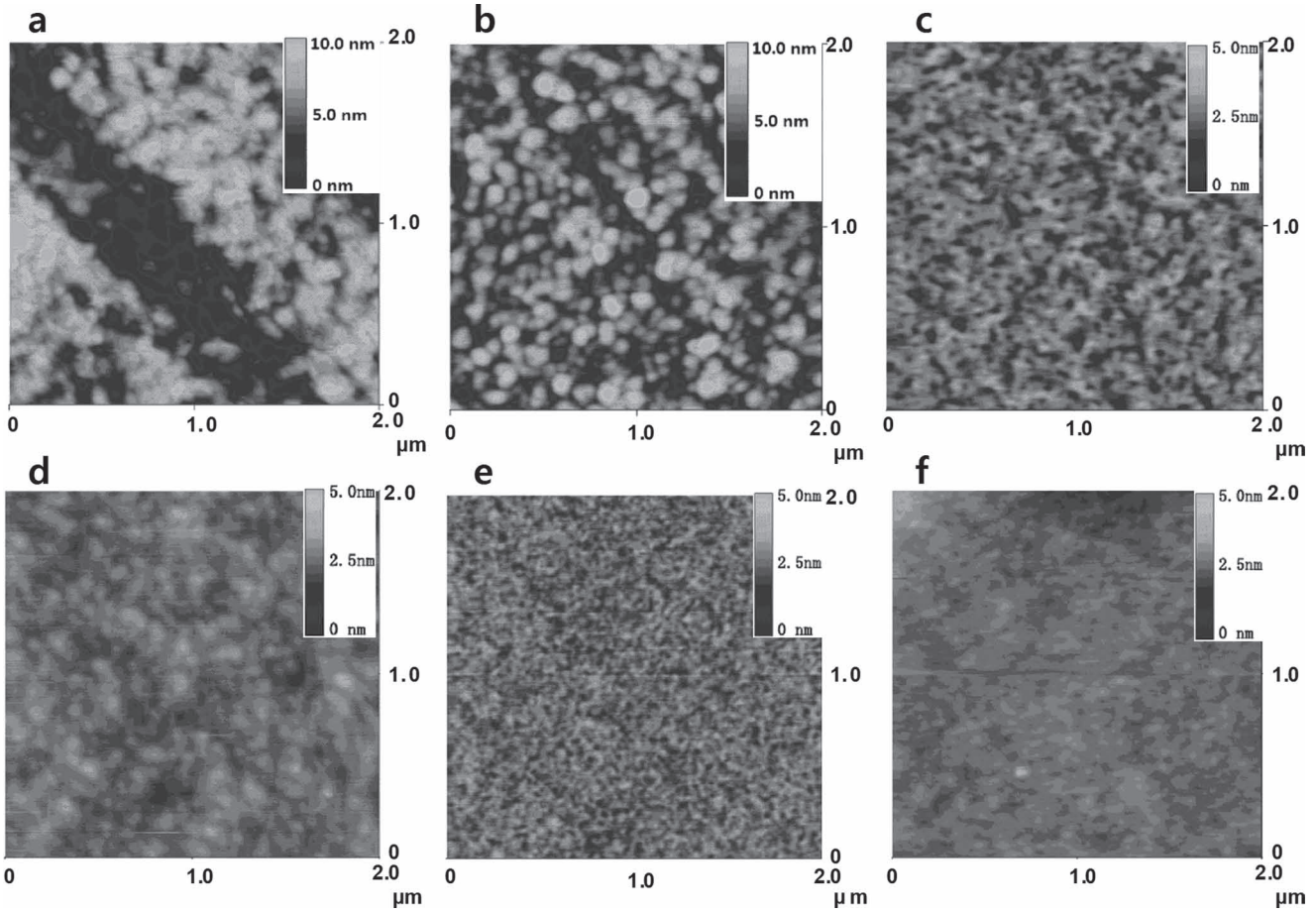

Figure 7. Morphology of blend films spin coated from chlorobenzene as imaged by tapping mode AFM: a) **F1**/$PC_{61}BM$ (1:2 weight ratio); b) **F2**/$PC_{61}BM$ (1:2 weight ratio); c) **20**/$PC_{61}BM$ (1:2 weight ratio); d) **F3**/$PC_{61}BM$ (1:2 weight ratio); e) **F4**/$PC_{61}BM$ (1:2 weight ratio); and f) **F5**/$PC_{61}BM$ (1:2 weight ratio).

photons in the similar wavelength range with maximum external quantum efficiency (EQE) at about 400 nm. The incident photon to current efficiency (IPCE) was enhanced from 400 nm to 700 nm when $PC_{71}BM$ is used. As observed for devices containing FHBC derivatives studied previously,[9] the results for this set of FHBC derivatives suggest there is still potential for improvement in device performance. In order to achieve higher efficiencies, a balance between light harvesting capacity, energy levels and donor-acceptor blend morphology is essential. With this in mind, further studies into FHBC-based materials are in progress with the aim to reach higher power conversion efficiency in single active layer small molecule BHJSC devices.

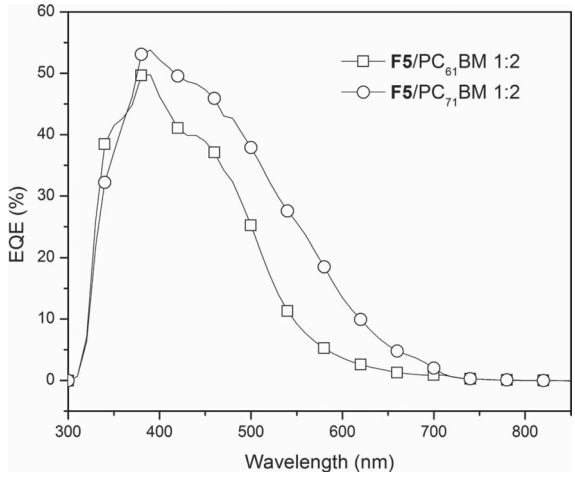

Figure 8. Spectral response of devices containing **F5** as donor and $PC_{61}BM$ or $PC_{71}BM$ as acceptor.

3. Conclusions

A series of well-defined solution processable FHBC compounds and FHBC-TBT hybrids have been successfully synthesised, fully characterized and applied in small-molecule BHJ solar cells. Solubility of the FHBC compounds was improved with the increasing of the number of 9,9-dialkylfluorene unit attached. Photophysical and electrochemical measurements revealed that the introduction of the TBT unit effectively broadened light absorption and lowered the HOMO-LUMO energy gap of the FHBC compounds. While the LUMO energy level of the compounds was lowered, the HOMO level was more or

less maintained. All the FHBC compounds show strong self-association of the HBC core in both solution and the solid state, evidenced by concentration-dependent NMR and XRD studies respectively. In AFM experiments, nanoscale phase separation was observed in thin films of FHBC and $PC_{61}BM$ blends. BHJSCs devices with these compounds as donors were fabricated. FHBC compounds with a TBT unit showed higher J_{sc} and similar V_{oc} compared with compounds without TBT. With $PC_{61}BM$ as acceptor, power conversion efficiency of 1.12% was achieved with **F4** as the donor material in the unoptimized BHJSCs devices under the simulated solar illumination. The efficiency was increased to 1.64% when $PC_{71}BM$ was used as the acceptor and **F5** as the donor, with a maximum EQE of 54% at about 400 nm. Although the overall power conversion efficiency of the BHJSCs studied here is still moderate, the concept of combining highly absorbing unit TBT with FHBC unit proves to be helpful in terms of improving device performance. Further optimization of material design and device fabrication conditions are currently under investigation.

4. Experimental Section

General: All reactions were performed using anhydrous solvent under an inert atmosphere unless stated otherwise. Silica gel (Merck 9385 Kieselgel 60) was used for flash chromatography. Thin layer chromatography was performed on Merck Kieselgel 60 silica gel on glass (0.25 mm thick). ^{1}H and ^{13}C NMR spectra were recorded on a Varian Inova 500 spectrometer using $CDCl_3$ as solvent and TMS as internal standard. All ^{13}C NMR were proton decoupled. Mass spectra were recorded with matrix-assisted laser desorption/ionization time-of-flight mass spectrometry (MALDI-TOF MS; Bruker Reflex 2, trans-2-[3-(4-tert-butylphenyl)-2-methyl-2-propenylidene]malononitrile as matrix) spectrometer. IR spectra were obtained on a Perkin Elmer Spectrum One Fourier transform infrared (FTIR) spectrometer while UV-vis spectra were recorded using a Cary 50 UV-vis spectrometer. PL was measured with a Varian Cary Eclipse fluorimeter. Melting points were determined on a Büchi 510 melting point apparatus. Note: All FHBC derivatives reported here were solids with no melt behavior observed below 250 °C. Elemental analyses were obtained on a Perkin-Elmer EA 2400 (for C, H) and commercially through CMAS, Victoria. Compounds **3**,[16] **4**,[17] **18**,[9a] **19**,[9d] **20**,[9c] and **21**[11] have been reported in the literature. All the other starting compounds and reagents were commercially available.

BHJ Solar Cell Device Fabrication and Testing: PEDOT:PSS (Baytron P AI4083) was spin-coated (5000 rpm) on patterned ITO glasses, which were washed by detergent, deionized water, methanol, acetone, and 2-propanol in an ultrasonication bath and UV/ozone-treated. The films were baked at 150 °C for 5 min in air. Solution of FHBC compounds and $PC_{61}BM$ (25 mg mL^{-1}) were prepared in chlorobenzene separately. The solutions were stirred at 60 °C for 2 h and cooled to room temperature before they were mixed together. Blend solutions (donor:acceptor 1:2) were made by mixing appropriate volumes of the solutions. The resulting solutions were stirred for 30 min and spin-coated (1500 rpm) on the PEDOT:PSS films. TiO_x precursor solution (1:200 in methanol) was deposited on the active layer by spin-coating (2000 rpm) to form ≈10 nm of TiO_x layer. The films were exposed to air for about 20 min at room temperature for hydrolysis and then transferred to a metal evaporation chamber and aluminium (100 nm) was deposited through a shadow mask (active area was 0.20 cm^2) at approximately 1×10^{-6} Torr. Film thickness was determined by Veeco Dektak 150+ Surface Profiler. The solar cells were illuminated at 100 mW cm^{-2} using 1 kW Oriel solar simulator with an AM 1.5G filter in air and current density–voltage (*J*–*V*) curves were measured using a Keithley 2400 source measurement unit. For accurate measurement, the light intensity was calibrated using a reference silicon solar cell (PVmeasurements Inc.) certified by the National Renewable Energy Laboratory. Spectral response was measured with a Keithley 2400 source meter, using monochromatic light from a Xe lamp in combination with monochromator (Oriel, Cornerstone 130). A calibrated Si cell was used as reference.

Synthesis of (9,9-Dioctyl-7-(4-(phenylethynyl)phenyl)-9H-fluoren-2-yl) trimethylsilane (***5***): To a flame-dried Schlenk tube (100 mL) were charged **3** (2.57 g, 10 mmol), compound **4** (6.5 g, 11 mmol) and $Pd(PPh_3)_4$ (0.58 g, 0.5 mmol) against N_2 flow, followed by the addition of degassed toluene (100 mL) and aqueous Et_4NOH solution (20% wt, 20 mL). The reaction mixture was then heated at 90 °C for 16 h, cooled to ambient and extracted with toluene. The organic phase was washed with water and concentrated by evaporation. The residue was purified by column chromatography on silica gel using petroleum spirit/dichloromethane (4:1) as eluent. Compound **5** was obtained as yellowish crystals after recrystallization from petroleum spirits and ethanol (2.4 g, 75%). ^{1}H NMR (500 MHz, $CDCl_3$): δ (ppm) 7.83 (m, 2H, Ar*H*), 7.76 (m, 5H, Ar*H*), 7.72 (m, 5H, Ar*H*), 7.44 (m, 3H, Ar*H*), 2.15 (m, 4H, -C*H*$_2$-), 1.25 (m, 20H, -C*H*$_2$-), 0.96 (t, 6H, -CH$_3$), 0.86 (m, 4H, -C*H*$_2$-), 0.48 (s, 9H, -C*H*$_3$). ^{13}C NMR (125 MHz, $CDCl_3$): δ (ppm) 152.54, 150.99, 142.24, 142.11, 141.64, 140.04, 139.98, 132.88, 132.73, 132.46, 129.16, 128.39, 127.83, 126.75, 124.24, 122.83, 122.09, 121.03, 120.02, 90.99, 90.39, 55.96, 41.02, 32.61, 30.74, 29.97, 29.92, 24.59, 23.45, 14.92. FT-IR (neat): λ (cm^{-1}) 2925, 2354, 1597, 1464, 1403, 1247, 1091, 770. HRMS (ESI): *m/z* = 638.43017 M$^+$, (calcd. for $C_{40}H_{58}Si$: 638.43023). Elemental analysis: calcd. for $C_{40}H_{58}Si$, C, 86.5; H, 9.2; found, C, 87.0; H, 9.3.

Synthesis of Compound ***7***: Compound **5** (0.639 g, 1 mmol) and compound **6** (0.38 g, 1 mmol) were dissolved in diphenyl ether (2 mL) and heated at 260 °C for 24 h. Compound **7** (0.61 g, 61% yield) was isolated as a white solid after column chromatography (SiO_2, dichloromethane/petroleum spirits 1:4). ^{1}H NMR (500 MHz, $CDCl_3$): δ (ppm) 7.66 (m, 2H, Ar*H*), 7.47 (m, 2H, Ar*H*), 7.42 (m, 2H, Ar*H*), 7.22 (d, 2H, Ar*H*), 6.92 (m, 27H, Ar*H*), 1.95 (m, 4H, -C*H*$_2$-), 1.13 (m, 20H, -C*H*$_2$-), 0.83 (t, 6H, -CH$_3$), 0.72 (m, 4H, -C*H*$_2$-), 0.33 (s, 9H, -C*H*$_3$). ^{13}C NMR (125 MHz, $CDCl_3$): δ (ppm) 152.32, 150.95, 142.27, 141.50, 141.33, 141.25, 140.84, 140.74, 140.40, 139.62, 138.89, 132.71, 132.60, 132.34, 128.44, 127.55, 126.49, 126.10, 126.04, 121.89, 120.61, 119.76, 55.84, 40.93, 32.61, 30.76, 29.99, 29.91, 24.56, 23.45, 14.93. FTIR (neat): λ (cm^{-1}) 2925, 1601, 1464, 1400, 1248, 1092, 838. HRMS (ESI): *m/z* = 994.58685 M$^+$, (calcd. for $C_{74}H_{78}Si$: 994.58673). Elemental analysis: calcd. for $C_{74}H_{78}Si$, C, 89.3; H, 7.9; found, C, 90.3; H, 8.2.

Synthesis of Compound ***8***: To a solution of Compound **7** (0.2 g, 0.2 mmol) in dichloromethane (10 mL) at 0 °C was added dropwise iodine monochloride (1 M in dichloromethane, 0.25 mL). After being stirred for 2 h at room temperature, the reaction mixture was poured into 50 mL of 10% aqueous $Na_2S_2O_4$ solution. The mixture was extracted with dichloromethane and dried over Na_2SO_4. The organic phase was filtered through a plug of silica and concentrated by evaporation. Compound **8** (0.195 g, 93% yield) was obtained as a white solid after precipitation in methanol. ^{1}H NMR (500 MHz, $CDCl_3$): δ (ppm) 7.63 (m, 3H, Ar*H*), 7.40 (m, 3H, Ar*H*), 7.21 (d, 2H, Ar*H*), 6.92 (m, 27H, Ar*H*), 1.92 (m, 4H, -C*H*$_2$-), 1.18 (m, 20H, -C*H*$_2$-), 0.84 (t, 6H, -C*H*$_3$), 0.62 (m, 4H, -C*H*$_2$-). ^{13}C NMR (125 MHz, $CDCl_3$): δ (ppm) 153.38, 150.65, 140.65, 140.50, 140.38, 139.80, 138.99, 137.83, 135.79, 132.03, 131.90, 131.49, 131.42, 126.70, 126.59, 125.89, 125.23, 125.21, 121.36, 120.92, 119.80, 92.28, 55.37, 40.19, 31.76, 29.91, 29.18, 29.11, 23.66, 22.61, 14.10. FTIR (neat): λ (cm^{-1}) 2922, 1736, 1601, 1457, 1377, 1263, 1157, 698. HRMS (ESI): *m/z* = 1048.44337 M$^+$, (calcd. for $C_{71}H_{69}I$: 1048.44385). Elemental analysis: calcd. for $C_{71}H_{69}I$, C, 81.3; H, 6.6; found, C, 80.6; H, 6.5.

Synthesis of Compound ***10***: This compound was synthesized by a similar procedure used for compound **5** in a yield of 96%. ^{1}H NMR (500 MHz, $CDCl_3$): δ (ppm) 7.35-7.68 (m, 12H, Ar*H*), 7.15 (m, 2H, Ar*H*), 6.81 (m, 27H, Ar*H*), 1.93 (m, 8H, -C*H*$_2$-), 1.11 (m, 40H, -C*H*$_2$-), 0.72 (m, 20H, -C*H*$_2$, -C*H*$_3$), 0.25 (s, 9H, -C*H*$_3$). ^{13}C NMR (125 MHz, $CDCl_3$): δ (ppm) 152.56, 152.42, 151.04, 142.29, 141.54, 141.51, 141.31, 141.11, 140.84, 140.76, 140.62, 140.53, 140.46, 139.80, 138.90, 132.75, 132.37, 132.31, 127.58, 127.46, 126.12, 126.09, 122.35, 121.91, 120.83, 120.70, 120.58, 119.85, 56.09, 55.96, 41.20, 41.01, 32.65, 30.88, 30.80, 30.07, 30.02,

29.98, 24.67, 23.47, 23.46, 14.94. FTIR (neat): λ (cm^{-1}) 2920, 1737, 1460, 1377, 1248, 1092, 698. HRMS (ESI): m/z = 1382.90086 M^+, (calcd. for $C_{103}H_{118}Si$: 1382.90028). Elemental analysis: calcd. for $C_{103}H_{118}Si$, C, 89.4; H, 8.6; found, C, 89.9; H, 8.9.

Synthesis of Compound ***11***: This compound was synthesized by a similar procedure used for compound **8** in a yield of 87%. ^{1}H NMR (500 MHz, $CDCl_3$): δ (ppm) 7.50-7.67 (m, 9H, Ar*H*), 7.34-7.40 (m, 3H, Ar*H*), 7.15 (m, 2H, Ar*H*), 6.81 (m, 27H, Ar*H*), 1.92 (m, 8H, -CH_2-), 1.04 (m, 40H, -CH_2-), 0.66 (m, 20H, -CH_2, -CH_3). ^{13}C NMR (125 MHz, $CDCl_3$): δ (ppm) 153.45, 151.75, 151.54, 150.89, 142.21, 140.67, 140.63, 140.49, 140.40, 140.17, 140.14, 139.87, 139.76, 139.65, 139.22, 138.00, 135.88, 132.11, 131.90, 131.50, 131.44, 126.71, 126.59, 126.22, 126.08, 125.80, 125.25, 121.43, 121.36, 121.06, 120.01, 119.87, 119.76, 92.41, 55.46, 55.23, 40.31, 40.22, 31.78, 31.76, 30.00, 29.93, 29.20, 29.17, 29.14, 23.81, 23.75, 22.61, 22.59, 14.08. FT-IR (neat): λ (cm^{-1}) 2924, 1884, 1455, 1377, 1264, 1073, 808, 696. HRMS (ESI): m/z = 1436.75762 M^+, (calcd. for $C_{100}H_{109}I$: 1436.75740). Elemental analysis: calcd. for $C_{100}H_{109}I$, C, 83.5; H, 7.6; found, C, 83.4; H, 7.6.

Synthesis of Compound ***12***: Compound **11** (0.144 g, 0.1 mmol) was dissolved in 300 mL of dry dichloromethane and the solution was purged with argon for 60 min before $FeCl_3$ (0.292 g, 1.8 mmol) in 2 mL of dry $MeNO_2$ was added. The reaction mixture was stirred for 5 h at 20 °C under argon purging before quenched by the adding of 200 mL of methanol. Dichloromethane was removed in reduced pressure and the precipitate was filtered and redissolved in hot chloroform. The solution was passed through a silica plug and precipitated again in MeOH. Compound **12** was obtained as a yellow solid in a yield of 85%. ^{1}H NMR (500 MHz, $CDCl_3$): δ (ppm) 8.13-7.61 (br, 24H, Ar*H*), 6.73-7.40 (m, 5H, Ar*H*), 2.06-2.41 (m, 8H, -CH_2-), 1.20 (m, 40H, -CH_2-), 0.82 (m, 20H, -CH_2, -CH_3). MALDI-TOF MS: m/z = 1424.8 M^+, (calcd. for $C_{100}H_{97}I$: 1424.7). FT-IR (neat): λ (cm^{-1}) 2926, 1740, 1455, 1366, 1218, 770. Elemental analysis: calcd. for $C_{100}H_{97}I$, C, 84.2; H, 6.9; found, C, 84.3; H, 6.7.

Synthesis of Compound ***13***: The mixture of compound **12** (100 mg, 0.07 mmol), 4,4,4′,4′,5,5,5′,5′-octamethyl-2,2'-bi(1,3,2-dioxaborolane) (50 mg, 0.2 mmol) and potassium acetate (100 mg, 1 mmol) was dried with high-vacuum at 60 °C for 1 h before 10 mL of DMF was added. Then, the solution was purged with N_2 for 30 min before the palladium catalyst was added. The reaction mixture was heated up to 85 °C and stirred overnight. After cooling to 20 °C, the reaction was quenched with methanol (50 mL) and the mixture was filtered through a plug of celite. The solid collected was removed from the filter by dissolution in hot chloroform. Solvent was removed under reduced pressure and the residue was precipitated in methanol. Compound **13** was obtained as a dark-green solid in a yield of 71%. ^{1}H NMR (500 MHz, $CDCl_3$): δ (ppm) 8.11-7.62 (br, 24H, Ar*H*), 6.73-7.40 (m, 5H, Ar*H*), 2.06-2.41 (m, 8H, -CH_2-), 1.55 (s, 12H, -CH_3), 1.30 (m, 40H, -CH_2-), 0.86 (m, 20H, -CH_2, -CH_3). MALDI-TOF MS: m/z = 1425.0 M^+, (calcd. for $C_{106}H_{109}BO_2$: 1424.9). FT-IR (neat): λ (cm^{-1}) 2918, 2153, 1735, 1609, 1375, 1084, 817, 668. Elemental analysis: calcd. for $C_{106}H_{109}BO_2$, C, 89.3; H, 7.7; found, C, 89.5; H, 7.7.

Synthesis of Monosubstituted FHBC ***F1***: Compound **12** (100 mg, 0.07 mmol) was dissolved in 50 mL of dry THF and the mixture was cooled to –78 °C. n-BuLi (2.5 M in hexane, 0.2 mL, 0.5 mmol) was added dropwise and the mixture was stirred at –78°C for 1 h. Then, 2 mL of methanol was added and the mixture was warmed up to room temperature. THF was removed in reduced pressure and the residue was redissolved in chloroform and passed through a plug of silica. After precipitated in methanol, Compound **14** was obtained as a yellow solid in a yield of 90%. ^{1}H NMR (500 MHz, $CDCl_3$): δ (ppm) 8.11-7.62 (m, 25H, Ar*H*), 7.02-7.45 (m, 5H, Ar*H*), 2.06-2.47 (m, 8H, -CH_2-), 1.05-1.48 (br, 40H, -CH_2-), 0.88 (m, 20H, -CH_2, -CH_3). MALDI-TOF MS: m/z = 1298.9 M^+, (calcd. for $C_{100}H_{98}$: 1298.8). FTIR (neat): λ (cm^{-1}) 2926, 1738, 1466, 1367, 1218, 768. Elemental analysis: calcd. for $C_{100}H_{98}$, C, 92.4; H, 7.6. found, C 92.2; H, 7.7.

Synthesis of Compound ***14***: This compound was synthesized by a similar procedure used for compound **5** in a yield of 96%. ^{1}H NMR (500 MHz, $CDCl_3$): δ (ppm) 7.36-7.73 (m, 18H, Ar*H*), 7.15 (m, 2H, Ar*H*), 6.80 (m, 27H, Ar*H*), 1.95 (m, 12H, -CH_2-), 1.05 (br, 60H, -CH_2-), 0.65-0.75 (br, 30H, -CH_2, -CH_3), 0.25 (s, 9H, -CH_3). ^{13}C NMR (125 MHz, $CDCl_3$): δ (ppm) 152.60, 152.55, 152.38, 151.00, 142.25, 141.50, 141.46, 141.32, 141.27, 141.23, 141.21, 141.11, 140.84, 140.81, 140.71, 140.57, 140.51, 140.43, 139.78, 138.86, 132.72, 132.67, 132.33, 132.27, 128.48, 127.54, 127.42, 126.97, 126.94, 126.89, 126.84, 126.61, 126.08, 126.05, 126.03, 122.31, 122.28, 121.88, 120.82, 120.74, 120.69, 120.56, 119.83, 56.14, 56.06, 55.94, 41.20, 41.16, 40.98, 40.82, 32.61, 31.75, 30.85, 30.77, 30.71, 30.54, 30.03, 29.99, 29.95, 29.91, 29.82, 25.78, 24.73, 24.65, 24.48, 23.43, 14.90 FTIR (neat): λ (cm^{-1}) 2923, 1601, 1458, 1377, 1248, 1092, 814, 698. HRMS (ESI): m/z = 1771.21342 M^+, (calcd. for $C_{132}H_{158}Si$: 1771.21328). Elemental analysis: calcd. for $C_{132}H_{158}Si$, C, 89.4; H, 9.0; found, C, 90.3; H, 9.2.

Synthesis of Compound ***15***: This compound was synthesized by a similar procedure used for compound **8** in a yield of 87%. ^{1}H NMR (500 MHz, $CDCl_3$): δ (ppm) 7.60-7.82 (m, 15H, Ar*H*), 7.42-7.51 (m, 3H, Ar*H*), 7.23 (m, 2H, Ar*H*), 6.91 (m, 27H, Ar*H*), 1.92-2.08 (br, 12H, -CH_2-), 1.15 (br, 60H, -CH_2-), 0.70-0.85 (m, 30H, -CH_2, -CH_3). ^{13}C NMR (125 MHz, $CDCl_3$): δ (ppm) 153.44, 151.81, 151.75, 151.72, 151.54, 150.90, 141.18, 140.66, 140.62, 140.58, 140.47, 140.43, 140.39, 140.33, 140.23, 140.15, 140.03, 139.87, 139.70, 139.59, 139.25, 138.01, 135.87, 132.11, 131.88, 131.49, 131.43, 126.69, 126.57, 126.24, 126.13, 126.05, 125.77, 125.24, 125.21, 125.18, 121.48, 121.46, 121.43, 121.35, 121.04, 120.03, 119.94, 119.85, 119.72, 92.41, 55.46, 55.31, 55.22, 40.33, 40.22, 31.77, 30.92, 30.00, 29.93, 29.19, 29.16, 29.14, 23.89, 23.81, 23.75, 22.60, 22.58, 14.07, 14.04. FTIR (neat): λ (cm^{-1}) 2924, 1600, 1455, 1377, 1263, 1073, 809, 696. HRMS (ESI): m/z = 1825.07136 M^+, (calcd. for $C_{129}H_{149}I$: 1825.07040). Elemental analysis: calcd. For $C_{129}H_{149}I$, C, 84.8; H, 8.2; found, C, 85.4; H, 8.4.

Synthesis of Compound ***16***: This compound was synthesized by a similar procedure used for compound **12** in a yield of 85%. ^{1}H NMR (500 MHz, $CDCl_3$): δ (ppm) 7.54-8.03 (m, 30H, Ar*H*), 7.04-7.40 (m, 5H, Ar*H*), 2.02-2.42 (br, 12H, -CH_2-), 1.22 (m, 60H, -CH_2-), 0.88 (m, 30H, -CH_2, -CH_3). ^{13}C NMR (125 MHz, $CDCl_3$): δ (ppm) 153.47, 152.02, 151.93, 151.89, 150.96, 149.17, 148.20, 141.21, 140.71, 140.50, 140.36, 140.23, 139.33, 138.10, 136.17, 135.96, 135.91, 134.40, 132.18, 132.15, 128.51, 128.49, 128.45, 128.41, 128.38, 128.36, 128.32, 128.29, 128.26, 128.25, 128.22, 126.39, 126.30, 121.79, 121.65, 121.63, 121.58, 121.56, 121.46, 121.39, 120.19, 120.17, 120.09, 120.04, 119.91, 92.46, 55.53, 55.50, 55.44, 40.72, 40.45, 40.26, 31.97, 31.86, 31.81, 31.76, 30.39, 30.11, 29.97, 29.60, 29.51, 29.31, 29.29, 29.22, 29.20, 29.12, 29.09, 24.38, 24.00, 23.79, 22.75, 22.67, 22.64, 22.59, 22.57, 14.19, 14.14, 14.10, 14.06. FTIR (neat): λ (cm^{-1}) 2923, 1737, 1454, 1377, 1257, 1218, 763. MALDI-TOF MS: m/z = 1813.2 M^+, (calcd. for $C_{129}H_{137}I$: 1813.0). Elemental analysis: calcd. For $C_{129}H_{137}I$, C, 85.4; H, 7.6; found, C, 85.9; H, 7.7.

Synthesis of Compound ***17***: This compound was synthesized by a similar procedure used for compound **13** in a yield of 71%. ^{1}H NMR (500 MHz, $CDCl_3$): δ (ppm) 7.71-8.08 (m, 30H, Ar*H*), 6.72-751 (m, 5H, Ar*H*), 2.12-2.40 (br, 12H, -CH_2-), 1.26 (m, 72H, -CH_2-), 0.86 (m, 30H, -CH_2, -CH_3). ^{13}C NMR (125 MHz, $CDCl_3$): δ (ppm) 152.16, 151.99, 151.95, 151.86, 150.24, 143.85, 140.58, 140.14, 133.85, 128.95, 128.22, 128.18, 128.15, 128.10, 128.07, 128.05, 128.02, 128.01, 127.98, 127.96, 127.95, 127.93, 126.29, 126.10, 124.34, 124.31, 122.64, 122.56, 121.63, 121.56, 120.08, 120.03, 119.07, 118.19, 118.17, 118.10, 117.94, 117.90, 83.74, 77.27, 77.02, 76.77, 55.50, 55.45, 55.30, 40.49, 40.29, 31.99, 31.89, 31.83, 29.61, 29.52, 29.31, 29.25, 29.23, 24.99, 24.39, 24.03, 23.81, 22.77, 22.69, 22.64, 14.22, 14.16, 14.11. FTIR (neat): λ (cm^{-1}) 2925, 1731, 1609, 1460, 1356, 1258, 1081, 815, 763. MALDI-TOF MS: m/z = 1813.4 M^+, (calcd. for $C_{135}H_{149}BO_2$: 1813.2). Elemental analysis: calcd. For $C_{135}H_{149}BO_2$, C, 89.4; H, 8.3; found, C, 89.3; H, 8.3.

Synthesis of Monosubstituted FHBC ***F2***: This compound was synthesized by a similar procedure used for compound **F1** in a yield of 90%. ^{1}H NMR (500 MHz, $CDCl_3$): δ (ppm) 7.67-8.11 (m, 31H, Ar*H*), 6.96-7.43 (m, 5H, Ar*H*), 2.10-2.40 (br, 12H, -CH_2-), 1.27 (m, 72H, -CH_2-), 0.89 (m, 30H, -CH_2, -CH_3). ^{13}C NMR (125 MHz, $CDCl_3$): δ (ppm) 151.98, 151.94, 151.85, 151.65, 151.53, 151.04, 140.84, 140.64, 140.61, 140.53, 140.39, 140.07, 139.81, 139.80, 128.26, 128.24, 128.04, 127.99, 127.05, 127.01, 126.83, 126.68, 126.35, 126.33, 126.29, 126.25, 126.09, 124.44, 122.97, 122.64, 121.68, 121.58, 120.07, 120.05, 119.92, 119.74, 119.70,

119.67, 119.56, 119.54, 118.22, 118.01, 117.97, 117.95, 117.94, 117.89, 117.84, 55.50, 55.45, 55.22, 40.75, 40.73, 40.50, 40.43, 31.99, 31.88, 31.83, 30.40, 30.14, 30.08, 29.60, 29.52, 29.31, 29.25, 25.37, 24.40, 24.02, 23.88, 22.76, 22.68, 22.63, 14.22, 14.15, 14.10. FTIR (neat): λ (cm^{-1}) 2925, 1736, 1463, 1378, 1219, 767. MALDI-TOF MS: m/z = 1687.3 M^+, (calcd. for $C_{129}H_{138}$: 1687.1). Elemental analysis: calcd. For $C_{129}H_{138}$, C, 91.8; H, 8.2. found, C, 91.7; H, 8.2.

Synthesis of FHBC-TBT Derivative ***F3***: This compound was prepared by using standard Suzuki coupling procedure (as described for the synthesis of compound **5**) between boronic ester derivative **13** and TBT derivative **21**. The product was purified by column chromatography and precipitated in methanol as a dark-red solid in a yield of 50%. ^{1}H NMR (500 MHz, $CDCl_3$): δ (ppm) 8.08-7.66 (m, 26H, Ar*H*), 7.48 (d, 2H, Ar*H*), 7.05-7.28 (m, 6H, Ar*H*), 2.78 (t, 2H, -C*H*$_2$-), 2.72 (t, 2H, -C*H*$_2$-), 2.19-2.43 (br, 8H, -C*H*$_2$-), 1.77 (m, 2H, -C*H*$_2$-), 1.67 (m, 2H, -C*H*$_2$-), 1.31-1.19 (m, 52H, -C*H*$_2$-), 0.87 (m, 26H, -C*H*$_3$). ^{13}C NMR (125 MHz, $CDCl_3$): δ (ppm) 153.77, 153.47, 153.37, 151.51, 151.01, 150.97, 150.89, 150.84, 146.20, 144.45, 143.43, 140.01, 137.71, 135.86, 134.51, 133.65, 132.12, 132.10, 130.66, 130.55, 128.98, 128.66, 127.53, 127.48, 125.74, 124.90, 124.30, 124.26, 123.87, 122.01, 121.93, 121.91, 119.29, 119.25, 119.20, 119.18, 103.94, 76.24, 75.98, 75.73, 54.51, 54.45, 39.73, 39.58, 39.51, 30.96, 30.86, 30.61, 30.58, 29.11, 28.58, 28.48, 28.40, 28.29, 28.24, 28.13, 21.73, 21.66, 21.58, 21.54, 13.17, 13.13, 13.06, 13.04. FTIR (neat): λ (cm^{-1}) 2926, 2853, 1464, 1378, 1220, 771. MALDI-TOF MS: m/z = 1765.1 M^+, (calcd. for $C_{126}H_{128}N_2S_3$: 1764.9). Elemental analysis: calcd. For $C_{126}H_{128}N_2S_3$, C, 85.7; H, 7.3; N, 1.6. found, C, 85.6; H, 7.4; N, 1.4.

Synthesis of FHBC-TBT Derivative ***F4***: This compound was prepared by using standard Suzuki coupling procedure (as described for the synthesis of compound **5**) between boronic ester derivative **17** and TBT derivative **21**. The product was obtained as a dark-red solid in a yield of 86%. ^{1}H NMR (500 MHz, $CDCl_3$): δ (ppm) 8.04-7.66 (m, 32H, Ar*H*), 7.46 (d, 2H, Ar*H*), 7.05-7.28 (m, 6H, Ar*H*), 2.76 (t, 2H, -C*H*$_2$-), 2.71 (t, 2H, -C*H*$_2$-), 2.06-2.47 (br, 12H, -C*H*$_2$-), 1.78 (m, 2H, -C*H*$_2$-), 1.68 (m, 2H, -C*H*$_2$-), 1.32-1.196(m, 72H, -C*H*$_2$-), 0.87 (m, 36H, -C*H*$_3$). ^{13}C NMR (125 MHz, $CDCl_3$): δ (ppm) 154.42, 154.23, 152.03, 152.02, 151.96, 151.90, 142.96, 140.68, 133.12, 132.23, 131.53, 129.98, 129.66, 129.28, 128.49, 128.47, 128.43, 128.40, 128.38, 128.27, 128.25, 128.22, 128.17, 126.42, 126.41, 126.40, 126.37, 126.35, 126.34, 126.33, 126.27, 126.25, 125.90, 125.25, 124.82, 121.70, 121.67, 121.66, 121.61, 121.59, 121.57, 120.24, 120.23, 120.21, 120.19, 120.17, 120.15, 120.11, 120.09, 120.08, 120.05, 120.03, 120.01, 55.54, 55.47, 55.42, 40.50, 32.00, 31.89, 31.84, 31.63, 31.59, 30.81, 30.70, 30.41, 30.15, 30.08, 29.74, 29.62, 29.52, 29.41, 29.32, 29.27, 29.25, 29.18, 29.17, 29.14, 29.09, 29.07, 24.41, 24.03, 23.90, 23.88, 22.77, 22.69, 22.64, 22.59, 22.56, 14.22, 14.16, 14.10, 14.07, 14.05. FTIR (neat): λ (cm^{-1}) 2926, 2853, 1460, 1378, 1220, 770. MALDI-TOF MS: m/z = 2153.5 M^+, (calcd. for $C_{155}H_{168}N_2S_3$: 2153.2). Elemental analysis: calcd. for $C_{155}H_{168}N_2S_3$, C, 86.4; H, 7.9; N, 1.3. found, C, 86.3; H, 7.9; N, 1.3.

Synthesis of 2,11-Bis-Substituted FHBC-TBT Derivative ***F5***: This compound was prepared by using standard Suzuki coupling procedure (as described for the synthesis of compound **5**) between boronic ester derivative **19** and TBT derivative **21**. The product was obtained as a red solid in a yield of 85%. ^{1}H NMR (500 MHz, $CDCl_3$): δ (ppm) 8.36 (s, 4H, Ar*H*), 8.17 (s, 4H, Ar*H*), 7.92-7.71 (m, 17H, Ar*H*), 7.70-7.61 (m, 4H, Ar*H*), 7.55 (s, 2H, Ar*H*), 7.49 (d, 2H, Ar*H*), 7.34 (br, 3H, Ar*H*), 7.16 (d, 2H, Ar*H*), 2.82 (t, 4H, -C*H*$_2$-), 2.73 (t, 4H, -C*H*$_2$-), 2.35 (br, 8H, -C*H*$_2$-), 1.82 (m, 4H, -C*H*$_2$-), 1.67 (m, 4H, -C*H*$_2$-), 1.41-1.04 (br, 64H, -C*H*$_2$-), 0.86 (m, 32H, -C*H*$_3$). ^{13}C NMR (125 MHz, $CDCl_3$): δ (ppm) 154.43, 154.27, 152.03, 151.89, 145.53, 143.05, 141.79, 140.89, 140.80, 140.05, 134.70, 133.29, 132.27, 131.65, 130.02, 129.71, 129.30, 128.75, 128.74, 128.71, 127.52, 127.44, 126.97, 126.95, 126.94, 126.93, 126.92, 125.94, 125.38, 125.37, 125.09, 125.04, 125.02, 123.46, 122.60, 122.58, 121.87, 121.84, 121.83, 120.50, 120.47, 120.45, 120.41, 120.38, 120.36, 120.32, 118.77, 55.62, 40.77, 40.74, 40.73, 31.94, 31.90, 31.67, 31.62, 30.89, 30.73, 30.35, 29.82, 29.60, 29.56, 29.52, 29.47, 29.30, 29.18, 24.37, 24.37, 22.71, 22.64, 22.59, 14.15, 14.12, 14.08. FTIR (neat): λ (cm^{-1}) 2923, 2852, 1467, 1380, 1269, 1220, 814, 759. MALDI-TOF MS: m/z = 2234.6 M^+, (calcd. for $C_{152}H_{158}N_4S_6$: 2234.1). Elemental analysis: calcd. for $C_{152}H_{158}N_4S_6$, C, 81.8; H, 7.1; N, 2.5. found, C, 81.8; H, 7.3; N, 2.4.

Supporting Information

Supporting Information is available from the Wiley Online Library or from the author.

Acknowledgements

The authors thank the Australian Solar Institute (Fellowship to W.W.H.W. and project grant), the Australian Research Council (DP0877325), the Victorian State Government Department of Business Innovation (Victorian Science Agenda) and Department of Primary Industries (Energy Technology Innovation Strategy), the Commonwealth Scientific and Industrial Research Organisation and the University of Melbourne for supporting the Victorian Organic Solar Cells Consortium. The authors also thank the Australian Synchrotron for the use of the SAXS/WAXS beamline for the X-ray experiments presented in this work.

Received: September 9, 2011
Revised: December 6, 2011
Published online: March 16, 2012

[1] C. W. Tang, *Appl. Phys. Lett.* **1986**, *48*, 183.
[2] a) S. Gunes, H. Neugebauer, N. S. Sariciftci, *Chem. Rev.* **2007**, *107*, 1324; b) B. C. Thompson, J. M. J. Fréchet, *Angew. Chem. Int. Ed.* **2008**, *47*, 58.
[3] a) G. Yu, J. Gao, J. C. Hummelen, F. Wudl, A. J. Heeger, *Science* **1995**, *270*, 1789; b) J. J. M. Halls, C. A. Walsh, N. C. Greenham, E. A. Marseglia, R. H. Friend, S. C. Moratti, A. B. Holmes, *Nature* **1995**, *376*, 498.
[4] a) Y. Liang, Z. Xu, J. Xia, S.-T. Tsai, Y. Wu, G. Li, C. Ray, L. Yu, *Adv. Mater.* **2010**, *22*, E135; b) C. Piliego, T. W. Holcombe, J. D. Douglas, C. H. Woo, P. M. Beaujuge, J. M. J. Fréchet, *J. Am. Chem. Soc.* **2010**, *132*, 7595; c) T.-Y. Chu, J. Lu, S. Beaupré, Y. Zhang, J.-R. m. Pouliot, S. Wakim, J. Zhou, M. Leclerc, Z. Li, J. Ding, Y. Tao, *J. Am. Chem. Soc.* **2011**, *133*, 4250; d) S. C. Price, A. C. Stuart, L. Yang, H. Zhou, W. You, *J. Am. Chem. Soc.* **2011**, *133*, 4625; e) H. Zhou, L. Yang, A. C. Stuart, S. C. Price, S. Liu, W. You, *Angew. Chem. Int. Ed.* **2011**, *50*, 2995; f) H.-Y. Chen, J. Hou, S. Zhang, Y. Liang, G. Yang, Y. Yang, L. Yu, Y. Wu, G. Li, *Nat. Photonics* **2009**, *3*, 649.
[5] a) M. C. Scharber, D. Mühlbacher, M. Koppe, P. Denk, C. Waldauf, A. J. Heeger, C. J. Brabec, *Adv. Mater.* **2006**, *18*, 789; b) G. Dennler, M. C. Scharber, C. J. Brabec, *Adv. Mater.* **2009**, *21*, 1323.
[6] a) J. Roncali, *Acc. Chem. Res.* **2009**, *42*, 1719; b) S. Loser, C. J. Bruns, H. Miyauchi, R. o. P. Ortiz, A. Facchetti, S. I. Stupp, T. J. Marks, *J. Am. Chem. Soc.* **2011**, *133*, 8142; c) B. Walker, C. Kim, T.-Q. Nguyen, *Chem. Mater.* **2010**, *23*, 470; d) H. Shang, H. Fan, Y. Liu, W. Hu, Y. Li, X. Zhan, *Adv. Mater.* **2011**, *23*, 1554; e) B. Walker, A. B. Tamayo, X.-D. Dang, P. Zalar, J. H. Seo, A. Garcia, M. Tantiwiwat, T.-Q. Nguyen, *Adv. Funct. Mater.* **2009**, *19*, 3063; f) A. Leliège, P. Blanchard, T. o. Rousseau, J. Roncali, *Org. Lett.* **2011**, 3098; g) G. Wei, S. Wang, K. Sun, M. E. Thompson, S. R. Forrest, *Adv. Energy Mater.* **2011**, *1*, 184; h) B. Yin, L. Yang, Y. Liu, Y. Chen, Q. Qi, F. Zhang, S. Yin, *Appl. Phys. Lett.* **2010**, *97*, 023303.
[7] a) J. Wu, W. Pisula, K. Müllen, *Chem. Rev.* **2007**, *107*, 718; b) P. Herwig, C. W. Kayser, K. Müllen, H. W. Spiess, *Adv. Mater.* **1996**, *8*, 510; c) S. Ito, M. Wehmeier, J. D. Brand, C. Kubel, R. Epsch, J. P. Rabe, K. Müllen, *Chem. Eur. J.* **2000**, *6*, 4327; d) M. Kastler, W. Pisula, D. Wasserfallen, T. Pakula, K. Müllen, *J. Am. Chem. Soc.* **2005**, *127*, 4286.
[8] a) W. Pisula, A. Menon, M. Stepputat, I. Lieberwirth, U. Kolb, A. Tracz, H. Sirringhaus, T. Pakula, K. Müllen, *Adv. Mater.* **2005**,

17, 684; b) J. L. Li, M. Kastler, W. Pisula, J. W. F. Robertson, D. Wasserfallen, A. C. Grimsdale, J. S. Wu, K. Müllen, *Adv. Funct. Mater.* **2007**, *17*, 2528; c) L. Schmidt-Mende, A. Fechtenkötter, K. Müllen, E. Moons, R. H. Friend, J. D. MacKenzie, *Science* **2001**, *293*, 1119; d) Y. Yamamoto, T. Fukushima, Y. Suna, N. Ishii, A. Saeki, S. Seki, S. Tagawa, M. Taniguchi, T. Kawai, T. Aida, *Science* **2006**, *314*, 1761; e) J. P. Hill, W. Jin, A. Kosaka, T. Fukushima, H. Ichihara, T. Shimomura, K. Ito, T. Hashizume, N. Ishii, T. Aida, *Science* **2004**, *304*, 1481.

[9] a) W. W. H. Wong, D. J. Jones, C. Yan, S. E. Watkins, S. King, S. A. Haque, X. Wen, K. P. Ghiggino, A. B. Holmes, *Org. Lett.* **2009**, *11*, 975; b) W. W. H. Wong, C.-Q. Ma, W. Pisula, C. Yan, X. L. Feng, D. J. Jones, K. Müllen, R. A. Janssen, P. Bäuerle, A. B. Holmes, *Chem. Mater.* **2010**, *22*, 457; c) W. W. H. Wong, T. B. Singh, D. Vak, W. Pisula, C. Yan, X. L. Feng, E. L. Williams, K. L. Chan, Q. Mao, D. J. Jones, C.-Q. Ma, K. Müllen, P. Bäuerle, A. B. Holmes, *Adv. Funct. Mater.* **2010**, *20*, 927; d) W. W. H. Wong, T. Khoury, D. Vak, C. Yan, D. J. Jones, M. J. Crossley, A. B. Holmes, *J. Mater. Chem.* **2010**, *20*, 7005; e) W. W. H. Wong, C.-Q. Ma, W. Pisula, A. Mavrinskiy, X. Feng, H. Seyler, D. J. Jones, K. Müllen, P. Baeuerle, A. B. Holmes, *Chem. Eur. J.* **2011**, *17*, 5549; f) W. W. H. Wong, D. Vak, T. B. Singh, S. Ren, C. Yan, D. J. Jones, I. I. Liaw, R. N. Lamb, A. B. Holmes, *Org. Lett.* **2010**, *12*, 5000.

[10] a) L. Biniek, C. L. Chochos, N. Leclerc, G. Hadziioannou, J. K. Kallitsis, R. Bechara, P. Leveque, T. Heiser, *J. Mater. Chem.* **2009**, *19*, 4946; b) M. Svensson, F. Zhang, S. C. Veenstra, W. J. H. Verhees, J. C. Hummelen, J. M. Kroon, O. Inganäs, M. R. Andersson, *Adv. Mater.* **2003**, *15*, 988; c) N. Blouin, A. Michaud, D. Gendron, S. Wakim, E. Blair, R. Neagu-Plesu, M. Belletête, G. Durocher, Y. Tao, M. Leclerc, *J. Am. Chem. Soc.* **2007**, *130*, 732; d) A. J. Moulé, A. Tsami, T. W. Bünnagel, M. Forster, N. M. Kronenberg, M. Scharber, M. Koppe, M. Morana, C. J. Brabec, K. Meerholz, U. Scherf, *Chem. Mater.* **2008**, *20*, 4045; e) S. H. Park, A. Roy, S. Beaupre, S. Cho, N. Coates, J. S. Moon, D. Moses, M. Leclerc, K. Lee, A. J. Heeger, *Nat. Photonics* **2009**, *3*, 297; f) M.-H. Chen, J. Hou, Z. Hong, G. Yang, S. Sista, L.-M. Chen, Y. Yang, *Adv. Mater.* **2009**, *21*, 4238; g) N. Blouin, A. Michaud, M. Leclerc, *Adv. Mater.* **2007**, *19*, 2295.

[11] J.-J. Kim, H. Choi, J.-W. Lee, M.-S. Kang, K. Song, S. O. Kang, J. Ko, *J. Mater. Chem.* **2008**, *18*, 5223.

[12] C. J. Brabec, A. Cravino, D. Meissner, N. S. Sariciftci, T. Fromherz, M. T. Rispens, L. Sanchez, J. C. Hummelen, *Adv. Funct. Mater.* **2001**, *11*, 374.

[13] J. Wu, A. Fechtenkötter, J. Gauss, M. D. Watson, M. Kastler, C. Fechtenkötter, M. Wagner, K. Müllen, *J. Am. Chem. Soc.* **2004**, *126*, 11311.

[14] a) S. Laschat, A. Baro, N. Steinke, F. Giesselmann, C. Hägele, G. Scalia, R. Judele, E. Kapatsina, S. Sauer, A. Schreivogel, M. Tosoni, *Angew. Chem. Int. Ed.* **2007**, *46*, 4832; b) S. Sergeyev, W. Pisula, Y. H. Geerts, *Chem. Soc. Rev.* **2007**, *36*, 1902.

[15] M. M. Wienk, J. M. Kroon, W. J. H. Verhees, J. Knol, J. C. Hummelen, P. A. van Hal, R. A. J. Janssen, *Angew. Chem. Int. Ed.* **2003**, *42*, 3371.

[16] X. Zheng, M. E. Mulcahy, D. Horinek, F. Galeotti, T. F. Magnera, J. Michl, *J. Am. Chem. Soc.* **2004**, *126*, 4540.

[17] S. Ren, D. Zeng, H. Zhong, Y. Wang, S. Qian, Q. Fang, *J. Phys. Chem. B* **2010**, *114*, 10374.